

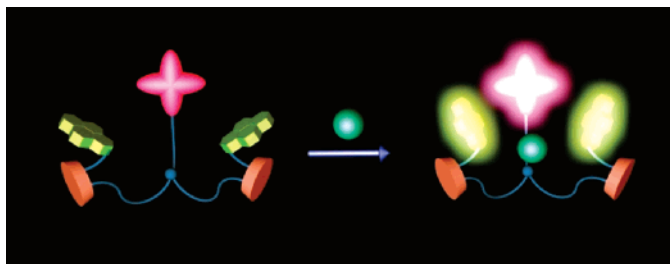
Calix[4]arene-Based, Hg²⁺-Induced Intramolecular Fluorescence Resonance Energy Transfer Chemosensor

Amel Ben Othman,^{†,‡} Jeong Won Lee,[§] Jia-Sheng Wu,[§] Jong Seung Kim,^{*,∇} Rym Abidi,[‡] Pierre Thuéry,[‡] Jean Marc Strub,[†] Alain Van Dorsselaer,[†] and Jacques Vicens^{*,†}

IPHC-ULP-ECPM-CNRS, 25 rue Becquerel, F-67087 Strasbourg Cédex, France, Department of Chemistry, Dankook University, Seoul 140-714, Korea, Department of Chemistry, Korea University, Seoul 130-701, Korea, Facultés des Sciences, Université de Bizerte, 7021 Zarzouna-Bizerte, Tunisia, and CEA/Saclay, SCM (CNRS URA 331), Bât. 125, F-91191 Gif-sur-Yvette, France

vicens@chimie.u-strasbg.fr; jongskim@korea.ac.kr

Received June 8, 2007



A novel calix[4]arene-based chemosensor **1** based on Hg²⁺-induced fluorescence resonance energy transfer (FRET) was synthesized, and its sensing behavior toward metal ions was investigated by UV/vis and fluorescence spectroscopies. Addition of Hg²⁺ to a CH₃CN solution of **1** gave a significantly enhanced fluorescence at ~575 nm via energy transfer (FRET-ON) from the pyrenyl excimer to a ring-opened rhodamine moiety. In contrast, addition of Al³⁺ induced a distinct increase of pyrenyl excimer emission (~475 nm), while no obvious FRET-ON phenomenon was observed. Different binding behaviors of **1** toward Hg²⁺ and Al³⁺ were also proposed for the interesting observation.

Introduction

Mercury has been known as a toxic metal since antiquity and has severe effects on human health and the environment.¹ Mercury contamination is widespread and arises from a variety of natural sources, such as oceanic and volcanic emissions,² as well as anthropogenic sources, such as gold mining and combustion of wastes and fossil fuels.³ Upon entering into the marine environment, bacteria convert inorganic mercury into methylmercury, which enters the food chain and bioaccumulates in higher organisms with involvement in mercury-pollution diseases.⁴

Given these environmental and toxicological concerns, efforts are being made to develop new mercury sensing strategies that can detect mercuric ion in the environment and in biological samples. Current techniques for Hg²⁺ screening (neutron

activation analysis, anodic stripping voltammetry, X-ray fluorescence spectrometry, inductivity coupled plasma mass spectrometry, etc.) usually require expensive and sophisticated instrumentation. Recently, a new approach involved in Hg²⁺ detection is the fluorescent chemosensor, which is receiving considerable interest because of its selectivity, sensitivity, and simplicity. A number of Hg²⁺-selective fluorescent chemosensors have been reported.⁵

The design of fluorescent chemosensors is mainly based on photoinduced electron/energy transfer (PET),⁶ metal–ligand charge transfer (MLCT),⁷ intramolecular charge transfer (ICT),⁸ excimer/exciple formation,⁹ imine isomerization,¹⁰ chelation-

(1) P. Weilhe edited a special issue of *Environmental Research* devoted to mercury and derivatives as toxic elements. Grandjean, P. *Environ. Res. Sect. A* **1998**, *77*, 67–178.

(2) (a) Renzoni, A.; Zino, F.; Franchi, E. *Environ. Res. Sect. A* **1998**, *77*, 68. (b) Malm, O. *Environ. Res. Sect. A* **1998**, *77*, 73. (c) Fitzgerald, W. F.; Lamborg, C. H.; Hammerschmidt, C. R. *Chem. Rev.* **2007**, *107*, 641.

(3) Boening, D. W. *Chemosphere* **2000**, *40*, 1335.

(4) Harris, H. H.; Pickering, I. J. P.; George, G. N. *Science* **2003**, *301*, 1203.

[†] IPHC-ULP-ECPM-CNRS.

[‡] Université de Bizerte.

[§] Dankook University.

[∇] Korea University.

[‡] CEA/Saclay, SCM (CNRS URA 331).

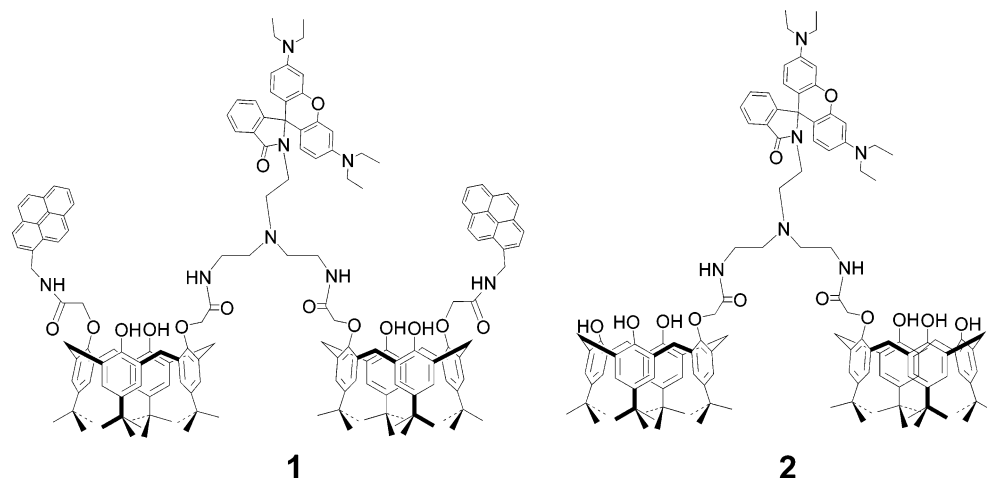
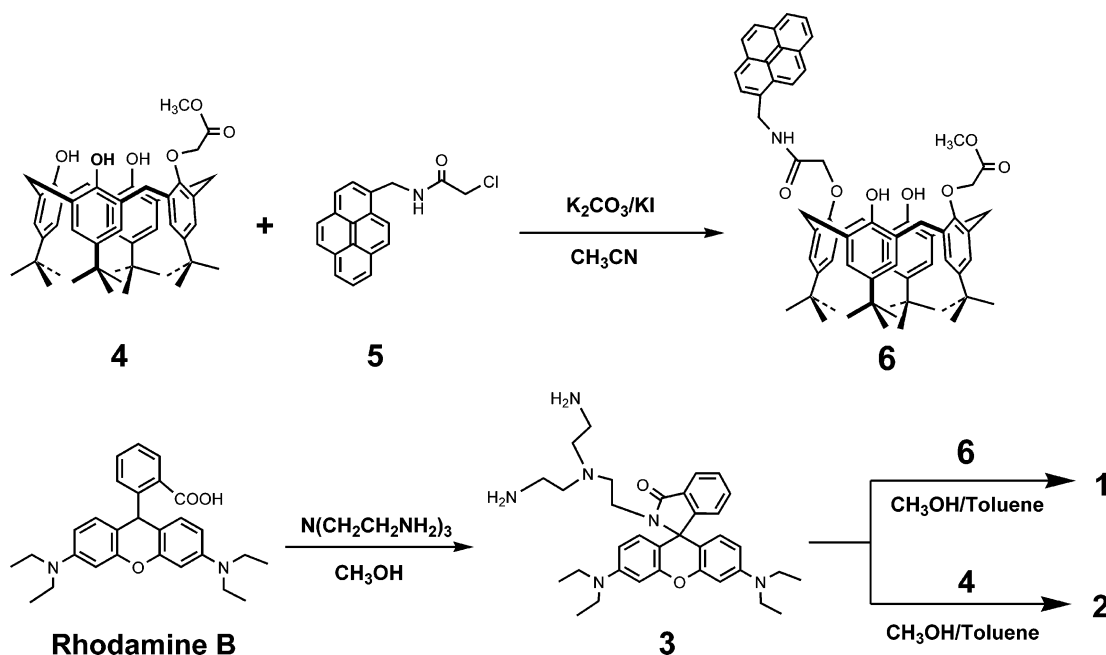


FIGURE 1. Structure of chemosensors 1 and 2.

SCHEME 1. Synthetic Pathways of 1 and 2



enhanced fluorescence (CHEF),¹¹ and fluorescence resonance energy transfer (FRET).¹² Currently, the FRET is an active field

in supramolecular chemistry due to its potential practical benefits in cell physiology, optical therapy, as well as selective and sensitive sensing toward targeted molecular or ionic species.¹³ FRET is defined as an excited-state energy interaction between two fluorophores in which an excited donor (D) transfers energy to an acceptor (A) without photoemission. Thus, FRET is required to have a certain degree of spectral overlap between

(5) (a) Descalzo, A. D.; Martínez-Manez, R.; Radeaglia, R.; Rurack, K.; Soto, J. *J. Am. Chem. Soc.* **2003**, *125*, 3418. (b) Nolan, E. M.; Lippard, S. J. *J. Am. Chem. Soc.* **2003**, *125*, 14270. (c) Matsushita, M.; Meijler, M. M.; Wirsching, P.; Lerner, R. A.; Jand, K. D. *Org. Lett.* **2005**, *7*, 4943. (d) Moon, S.-Y.; Youn, N. J.; Park, S. M.; Chang, S.-K. *J. Org. Chem.* **2005**, *70*, 2394. (e) Caballero, A.; Martínez, R.; Lloveras, V.; Ratera, I.; Vidal-Gancedo, J.; Würst, K.; Tarraga, A.; Molina, P.; Veciana, J. *J. Am. Chem. Soc.* **2005**, *127*, 15666. (f) Coskun, A.; Akkaya, E. U. *J. Am. Chem. Soc.* **2006**, *128*, 14474. (g) Zheng, H.; Qian, Z.-H.; Xu, L.; Yuan, F.-F.; Lan, L.-D.; Xu, J.-G. *Org. Lett.* **2006**, *8*, 859. (h) Zhu, X. J.; Fu, S. T.; Wong, W. K.; Guo, H. P.; Wong, W. Y. *Angew. Chem., Int. Ed.* **2006**, *45*, 3150. (i) Wu, J.-S.; Hwang, I.-C.; Kim, K. S.; Kim, J. S. *Org. Lett.* **2007**, *9*, 907. (j) Avirah, R. R.; Jyothish, K.; Ramaiah, D. *Org. Lett.* **2007**, *9*, 121.

(6) (a) Gunnlaugsson, T.; Davis, A. P.; O'Brien, J. E.; Glynn, M. *Org. Lett.* **2002**, *4*, 2449. (b) Vance, D. H.; Czarnik, A. W. *J. Am. Chem. Soc.* **1994**, *116*, 9397. (c) Kim, S. K.; Yoon, J. *Chem. Commun.* **2002**, 770.

(7) (a) Beer, P. D. *Acc. Chem. Res.* **1998**, *31*, 71. (b) Kim, M. J.; Konduri, R.; Ye, H.; MacDonnell, F. M.; Puntoriero, F.; Serroni, S.; Campagna, S.; Holder, T.; Kinsel, G.; Rajeshwar, K. *Inorg. Chem.* **2002**, *41*, 2471.

(8) (a) Xu, Z.; Xiao, Y.; Qian, X.; Cui, J.; Cui, D. *Org. Lett.* **2005**, *7*, 889. (b) Wang, J. B.; Qian, X. F.; Cui, J. N. *J. Org. Chem.* **2006**, *71*, 4308.

(9) (a) Nishizawa, S.; Kato, Y.; Teramae, N. *J. Am. Chem. Soc.* **1999**, *121*, 9463. (b) Wu, J.-S.; Zhou, J.-H.; Wang, P.-F.; Zhang, X.-H.; Wu, S.-K. *Org. Lett.* **2005**, *7*, 2133. (c) Schazmann, B.; Alhashimy, N.; Diamond, D. *J. Am. Chem. Soc.* **2006**, *128*, 8607.

(10) Wu, J.-S.; Liu, W.-M.; Zhuang, X.-Q.; Wang, F.; Wang, P.-F.; Tao, S.-L.; Zhang, X.-H.; Wu, S.-K.; Lee, S.-T. *Org. Lett.* **2007**, *9*, 33.

(11) Lim, N. C.; Schuster, J. V.; Porto, M. C.; Tanudra, M. A.; Yao, L.; Freaque, H. C.; Bruckner, C. *Inorg. Chem.* **2005**, *44*, 2018.

(12) (a) Serin, J. M.; Brousmiche, D. W.; Frechet, J. M. J. *J. Am. Chem. Soc.* **2002**, *124*, 11848. (b) Albers, A. E.; Okreglak, V. S.; Chang, C. J. *J. Am. Chem. Soc.* **2006**, *128*, 9640. (c) Lee, S. H.; Kim, S. K.; Bok, J. H.; Lee, S. H.; Yoon, J.; Lee, K.; Kim, J. S. *Tetrahedron Lett.* **2005**, *46*, 8163.

(d) Dichtel, W. R.; Serin, J. M.; Edler, C.; Frechet, J. M. J.; Matuszewski, M.; Tan, L.-S.; Ohulchanskyy, T. Y.; Prasad, P. N. *J. Am. Chem. Soc.* **2004**, *126*, 5380.

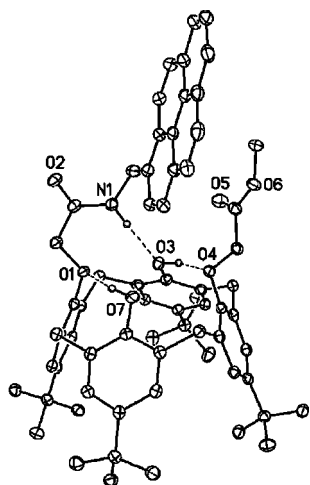


FIGURE 2. View of compound **6** in the solid state. Only hydrogen atoms involved in hydrogen bonds (dashed lines) are represented. Displacement ellipsoids are drawn at the 30% probability level.

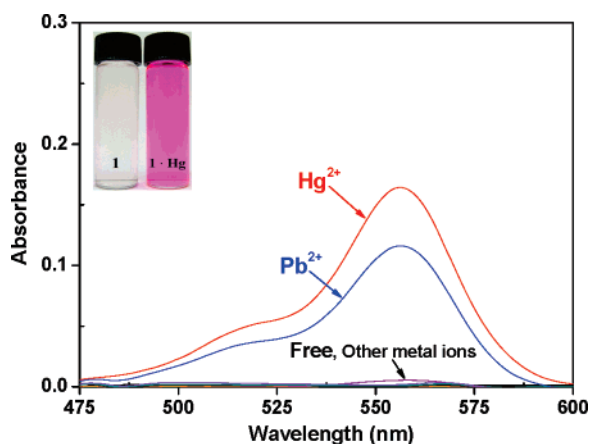


FIGURE 3. UV/vis spectra of **1** (0.015 mM) in CH₃CN in the presence of various metal cations, including Na⁺, K⁺, Rb⁺, Cs⁺, Mg²⁺, Pb²⁺, Ca²⁺, Hg²⁺, Sr²⁺, Ba²⁺, Fe²⁺, Co²⁺, Ag⁺, Cd²⁺, and Zn²⁺ (100 equiv, as perchlorates). Inset: Color change of **1** upon addition of Hg²⁺ ion.

the emission spectrum of the donor and the absorption spectrum of the acceptor. A variety of chemosensors have been reported based on a FRET signal mechanism.¹² For example, a dendrimer containing four coumarin laser dyes at the periphery and a perylenebis(dicarboximide) derivative at the core was described as a FRET sensor from the coumarin donor to the core acceptor.^{12a} Chang et al. reported the biological application of Ratio-PeroxyFluor-1 (RPF1) containing a two-fluorophore cassette, where the spectral overlap between coumarin donor and

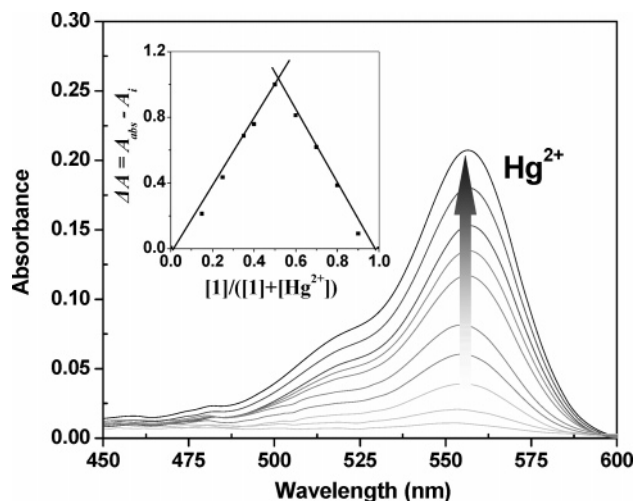


FIGURE 4. UV/vis spectra of **1** (0.015 mM) in CH₃CN upon addition of different concentrations of Hg(ClO₄)₂ (0, 0.0015, 0.0075, 0.015, 0.03, 0.075, 0.15, 0.225, and 0.3 mM, respectively). Job's plot for **1** vs. Hg²⁺. Absorption intensity is normalized.

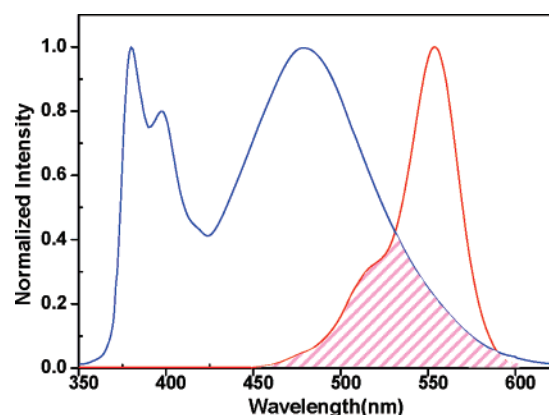


FIGURE 5. Spectral overlap between pyrenyl emission (blue) and ring-opened rhodamine B absorption (red).

fluoran/fluorescein acceptor partners could be controlled by the chemoselective peroxide-mediated deprotection of boronic ester pendants on the acceptor dye.^{12b} In addition, we also developed a new Pb²⁺-selective calix[4]crown chemosensor based on a dual signal of a hypsochromic shift of an azo group, as well as a fluorescence increase of the pyrenyl fluorophore via a suppressed FRET process.^{12c}

Calixarene has been widely exploited as the framework of many fluorescent chemosensors due to its flexible structural property.¹³ Our group has developed miscellaneous calixarene-structured chemosensors toward cations or anions for many years.¹⁴ However, as we note, FRET-based calixarene chemosensors had not received favorable interest, so far. Only a few cases are available.^{12c,15} Herein, we report a new calixarene-based FRET chemosensor **1** containing two pyrenyl groups (energy donor) and a rhodamine group (energy acceptor) as a new advance in this field. Compound **2** containing only rhodamine B was also synthesized for comparison (Figure 1). Addition of Hg²⁺ ion to the solution of **1** can lead to the ring-opening of the spirolactam unit in **1** with a FRET-ON signal mechanism.

Results and Discussion

Chemosensor **1** is a *N*-tripodal molecule consisting of two branched calixarene units (each bearing one amidopyrenylmethyl

(13) (a) Ji, H.-F.; Brown, G. M.; Dabestani, R. *Chem. Commun.* **1999**, 609. (b) Leray, I.; O'Reilly, F.; Habib Jiwan, J.-L.; Soumillion, J.-Ph.; Valeur, B. *Chem. Commun.* **1999**, 795. (c) Leray, I.; Lefevre, J.-P.; Delouis, J.-F.; Delaire, J.; Valeur, B. *Chem. Eur. J.* **2001**, 7, 4590. (d) Jin, T.; Ichikawa, K.; Koyama, T. *J. Chem. Soc. Chem. Commun.* **1992**, 499.

(14) (a) Kim, S. K.; Lee, S. H.; Lee, J. Y.; Lee, J. Y.; Bartsch, R. A.; Kim, J. S. *J. Am. Chem. Soc.* **2004**, 126, 16499. (b) Lee, S. H.; Kim, J. Y.; Ko, J.; Lee, J. Y.; Kim, J. S. *J. Org. Chem.* **2004**, 69, 2902. (c) Kim, M. J.; No, K.; Lee, J. H.; Yang, S. H.; Yu, S. H.; Cho, M. H.; Kim, J. S. *J. Org. Chem.* **2002**, 67, 3165. (d) Kim, H. J.; Kim, S. K.; Lee, J. Y.; Kim, J. S. *J. Org. Chem.* **2006**, 71, 6611. (e) Kim, J. S.; Shon, O. J.; Yang, S. H.; Kim, J. Y.; Kim, M. J. *J. Org. Chem.* **2002**, 67, 6514. (f) Kim, J. Y.; Kim, G.; Kim, C. R.; Lee, S. H.; Lee, J. H.; Kim, J. S. *J. Org. Chem.* **2003**, 68, 1933.

(15) Castellano, R. K.; Craig, S. L.; Nuckolls, C.; Rebek, J., Jr. *J. Am. Chem. Soc.* **2000**, 122, 7876.

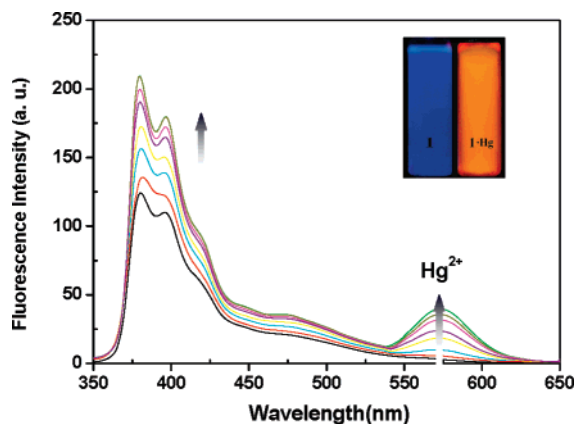


FIGURE 6. Fluorescence spectra of **1** (0.001 mM) in CH₃CN upon addition of increasing concentrations of Hg(ClO₄)₂ (0, 0.001, 0.01, 0.02, 0.03, 0.04, 0.05, and 0.06 mM) with an excitation at 343 nm.

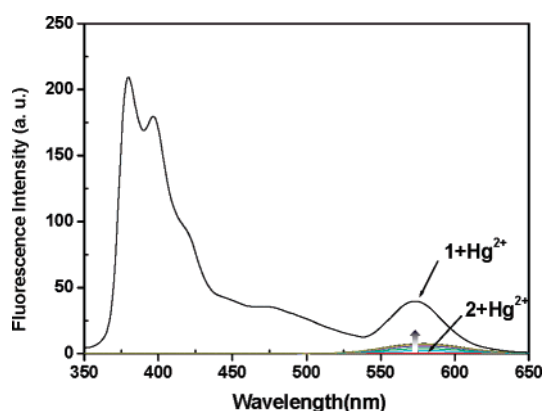


FIGURE 7. Fluorescence spectra of **1** (0.001 mM/CH₃CN) with 20 equiv of Hg(ClO₄)₂ and **2** (0.001 mM/CH₃CN) upon gradual addition of Hg(ClO₄)₂ (0, 0.001, 0.01, 0.02, 0.03, 0.04, 0.05, and 0.1 mM). Excitation at 343 nm.

moiety) and a rhodamine B unit (spirolactam form) in the vicinity of the pyrenyl groups. Compound **1** was designed as a Hg²⁺-induced FRET chemosensor mainly based on the following considerations: (i) the two pyrenyl groups in **1** are located at the rim of calixarene matrix with a flexible structure, which can easily lead to the formation of excimer emission (~475 nm); (ii) the excimer emission of pyrenyl and the absorption of ring-opened rhodamine have some spectral overlap, implying that **1** can be developed as a FRET chemosensor; (iii) the structures of tripodal tren (tris(2-aminoethyl)-amine moiety) and rhodamine spirolactam give a suitable binding structure for some specific cations; and (iv) the rhodamine structure can produce a sensitive OFF–ON optical signal when a recognition event takes place. In addition, the similar compound **2** without two pyrenyl groups was synthesized for comparative illustration of the FRET phenomenon. In our present work, addition of Hg²⁺ to a CH₃CN solution of **1** can result in an obvious occurrence of energy transfer from pyrenyl excimer (energy donor) to rhodamine (energy acceptor). In the absence of Hg²⁺ ion, energy transfer cannot take place due to the spirolactam structure of the rhodamine moiety, which constitutes a Hg²⁺-induced FRET chemosensor.

Preparation of **1** and **2** required the intermediate Tren-rhodamine **3**, which was obtained by reacting commercial rhodamine B with N(CH₂CH₂NH₂)₃ (Tren) in refluxing methanol with 79% yield (Scheme 1). To prepare **1**, the monomethyl

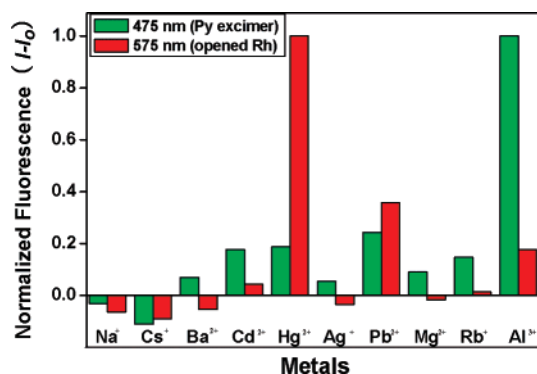


FIGURE 8. Bar profiles of normalized fluorescence changes ($I - I_0$) for **1** (0.001 mM) in CH₃CN upon addition of 100 equiv of various metal ions with an excitation at 343 nm. I_0 and I denote fluorescence intensity of **1** in the absence and presence of different metal cations (green: emission of pyrenyl excimer; red: emission of rhodamine B).

ester of *p*-*tert*-butyl-calix[4]arene **4** in the cone conformation was reacted with *N*-(1-pyrenylmethyl) chloroacetamide (**5**) in the presence of K₂CO₃/KI in refluxing CH₃CN to give monomethylester monoamido pyrenylmethyl *p*-*tert*-butylcalix[4]arene (**6**) in 38% yield. Intermediates **4** and **5** were synthesized according to reported procedures.^{16,17} Amidation reactions between **3** and **6** or **4** afforded **1** or **2** in 17% and 29% yields, respectively.

The structures of **1–3** and **6** were characterized by ¹H NMR, ¹³C NMR, MALDI-TOF MS, and elemental analysis. The spirolactam form of the rhodamine B units in **1–3** was confirmed by the presence of a peak at ~67.0 ppm in the ¹³C NMR spectra.¹⁸ The 1,3-O-di-linkages and the cone conformation of the calixarene units in **1**, **2**, and **6** were deduced from their ¹H NMR spectra presenting characteristic AB systems for the ArCH₂Ar protons.^{19,20} Further evidence for the cone conformation came from the ¹³C NMR peaks at ~31 ppm.²¹ Also, the cone conformation of **6** in the solid state was ascertained by single-crystal X-ray diffraction (Figure 2). Calixarene exists in the cone conformation with dihedral angles of 70.29(10)°, 45.60(14)°, 71.56(10)°, and 46.97(13)° between the four aromatic rings and the mean plane defined by the four methylenic bridges. The rings bearing the bulky substituents are more tilted with respect to the mean plane so as to move these groups further apart from each other. The phenolic oxygen atoms O3 and O7 are hydrogen bonded to their neighbors O4 and O1, respectively, whereas the N1H group is hydrogen bonded to O3. The pyrenyl group is planar within 0.064(5) Å and involved in a π – π stacking interaction with the pyrenyl of

(16) (a) Cheriaa, N.; Abidi, R.; Vicens, J. *Tetrahedron Lett.* **2005**, *46*, 1533. (b) Ben Othman, A.; Cheriaa, N.; Abidi, R.; Vicens, J.; Thuéry, P. *Acta Crystallogr. C* **2004**, *60*, 859.

(17) Kim, S. K.; Kim, S. H.; Kim, H. Y.; Lee, S. H.; Lee, S. W.; Ko, J.; Bartsch, R. A.; Kim, J. S. *Inorg. Chem.* **2005**, *44*, 7866.

(18) (a) Yang, Y.-K.; Yook, K.-J.; Tae, J. *J. Am. Chem. Soc.* **2005**, *127*, 16760. (b) Ramos, S. S.; Vilhena, A. F.; Santos, L.; Almeida, P. *Magn. Reson. Chem.* **2000**, *38*, 475.

(19) *Calixarenes: A Versatile Class of Macrocyclic Compounds*; Vicens, J., Böhrner, V., Eds.; Kluwer Academic Publishers: Dordrecht, Netherlands, 1991.

(20) We recently determined the X-ray structure of tren-*N*-dicalix resulting from the amidation reaction (under conditions very similar to those in this paper) of cone **4** with Tren showing that the cone conformation is maintained: Mahouachi, M.; Ben Othman, A.; Thuéry, P.; Kim, Y.; Lee, S. H.; Abidi, R.; Vicens, J. *J. Nano Biotechnol.* **2006**, *2*, 17.

(21) de Mendoza, J. C.; Prados, J.; Nieto, P.; Sanchez, P. N. *J. Org. Chem.* **1991**, *56*, 3372.

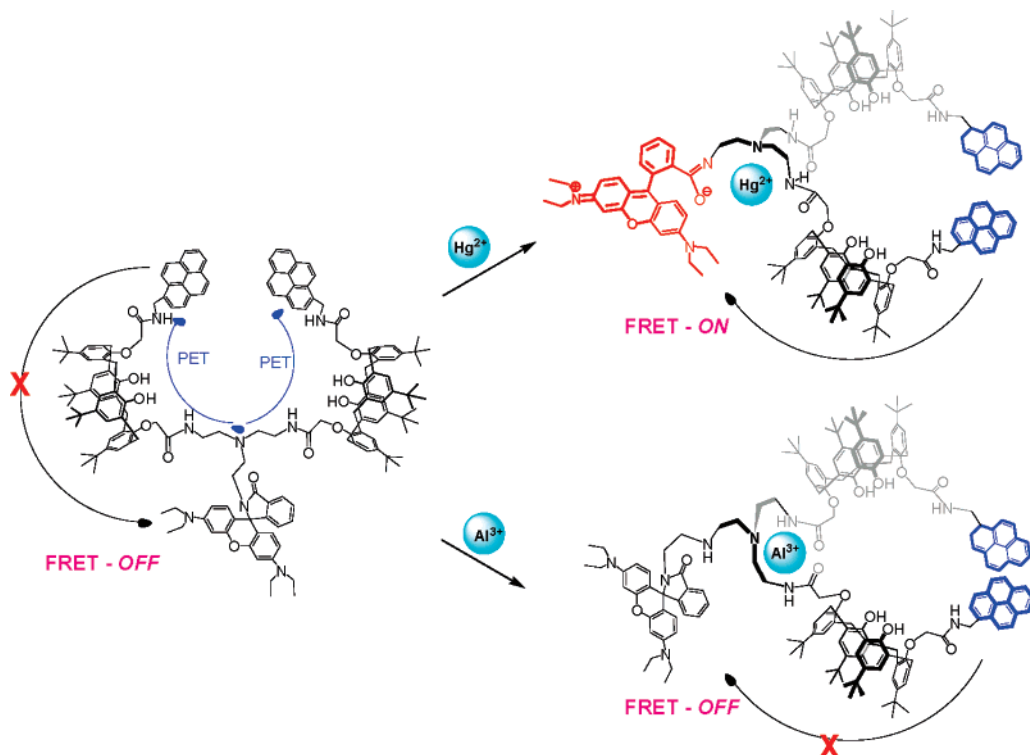


FIGURE 9. Proposed different complexation behaviors of **1** with Hg^{2+} and Al^{3+} .

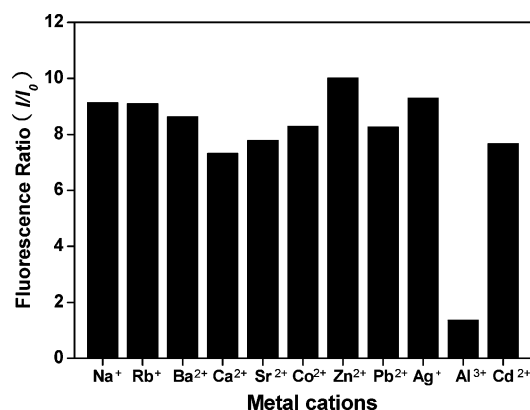


FIGURE 10. Fluorescence ratio at 575 nm of **1** (0.001 mM) in CH_3CN with 10 equiv of various coexisting metal cations in the presence and absence of 10 equiv of Hg^{2+} . I_0 and I denote fluorescence intensity of **1** + various cations in the absence and presence of Hg^{2+} .

a neighboring molecule related by the inversion center (the shortest $\text{C}\cdots\text{C}$ contact is 3.36 Å).

Variation of UV/vis spectra of **1** in CH_3CN in the presence of various metal perchlorates (Na^+ , K^+ , Rb^+ , Cs^+ , Mg^{2+} , Pb^{2+} , Ca^{2+} , Hg^{2+} , Sr^{2+} , Ba^{2+} , Fe^{2+} , Co^{2+} , Ag^+ , Cd^{2+} , and Zn^{2+}) is shown in Figure 3. Upon addition of 100 equiv of cations to the solution of **1**, only Hg^{2+} and Pb^{2+} lead to the appearance of a new absorption band centered at 555 nm. The Hg^{2+} induced a relatively larger change than did Pb^{2+} . This gives a visual color change from colorless to pink (inset of Figure 3). Other metal cations did not induce any distinct UV-vis spectra/color changes, implying that **1** shows a special binding ability toward Hg^{2+} and Pb^{2+} .

To further study the stoichiometry and association constant between **1** and Hg^{2+} , the UV/vis titration experiment was also carried out using 0.015 mM **1** in CH_3CN (Figure 4). The

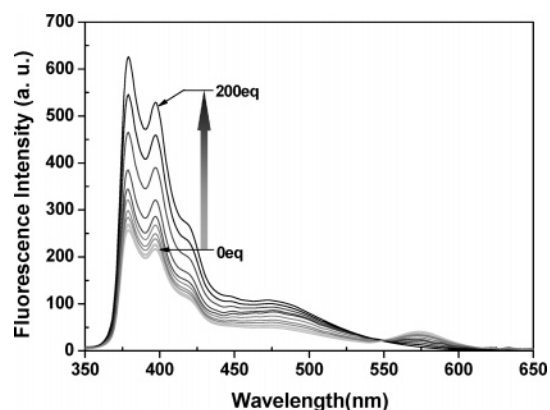


FIGURE 11. Fluorescence spectra of $\mathbf{1}\cdot\text{Hg}^{2+}$ (0.001 mM) in CH_3CN upon addition of increasing concentrations of $\text{Al}(\text{ClO}_4)_3$ (0, 0.0001, 0.0005, 0.001, 0.002, 0.005, 0.01, 0.02, 0.04, 0.06, 0.08, and 0.2 mM) with an excitation at 343 nm.

absorption peak at 555 nm increased upon gradual addition of Hg^{2+} and remained constant after 20 equiv of Hg^{2+} was added. A Job's plot analysis exhibited a maximum at 0.5 mol fraction of Hg^{2+} (inset of Figure 4), indicating the formation of 1:1 complex. The MALDI-TOF MS was conducted using a 10^{-3} M solution of **1** in CH_3CN with an excess of $\text{Hg}(\text{ClO}_4)_2$ to give the result of $m/z = 2746.216$ ($\mathbf{1} + \text{Hg}^{2+} + \text{K}^+ + \text{Na}^+ - 7\text{H}^+$), which gave further evidence of the formation of 1:1 complex between **1** and Hg^{2+} ion. Based on 1:1 stoichiometry and UV/vis titration data in Figure 4, an association constant of **1** with Hg^{2+} was found to be $39,070 \text{ M}^{-1}$.²²

(22) (a) Association constants were obtained using the computer program ENZFITTER, available from Elsevier-BIOSOFT, 68 Hills Road, Cambridge CB2 1LA, United Kingdom. (b) Connors, K. A. *Binding Constants, The Measurement of Molecular Complex Stability*; Wiley: New York, 1987.

Figure 5 shows the emission spectra of pyrenyl excimer (blue line) and the absorption spectra of rhodamine B (red line). Energy donor (pyrenyl excimer) and energy acceptor (rhodamine) have some spectral overlap, which makes FRET possible if the pyrenyl moiety is excited. When **1** is excited at 343 nm, the two pyrenyl groups give rise to not only monomer emission (<400 nm), but also excimer emission (~475 nm). The excited pyrenyl excimer can transfer energy to the ring-opened rhodamine moiety in its ground state, which leads to the radiative decay (~575 nm) of the rhodamine moiety. To confirm this FRET process, a series of fluorescence experiments were conducted.

Variation of the fluorescence spectra of **1** (0.015 mM) in CH₃CN with a function of the Hg²⁺ concentration is given in Figure 6. Upon gradual addition of Hg²⁺, the fluorescence intensities of the pyrenyl monomer (<400 nm), pyrenyl excimer (~475 nm), and rhodamine emission (575 nm) all increased when the excitation wavelength was at 343 nm. Obviously, the rhodamine emission comes from the FRET process of the pyrenyl excimer to rhodamine. However, according to the theory of FRET, pyrenyl excimer emission should decrease when such energy transfer takes place. In this case, the tren structure of **1** provides a tertiary *N* atom (containing an unshared electron pair), which quenches both the pyrenyl monomer and excimer emissions strongly in the absence of Hg²⁺ due to a PET process. However, when Hg²⁺ is added to the solution of **1**, PET is suppressed and the fluorescence is increased due to chelation-enhanced fluorescence (CHEF). For the complex **1**-Hg²⁺, CHEF may play a more important role than does FRET, thus enhanced fluorescence of both the pyrenyl monomer and excimer upon addition of Hg²⁺ is observed.

To further prove Hg²⁺-induced FRET of **1**, we prepared a similar compound **2** (only lacking the two pyrenyl groups) and tested its fluorescence changes in the presence of Hg²⁺. As shown in Figure 7, with an excitation wavelength at 343 nm, **2** exhibits a much smaller change of fluorescence upon addition of 100 equiv of Hg²⁺ ion compared with **1**, which indicates that energy transfer in **1** does take place from the pyrenyl excimer to rhodamine.

The effects of other metal cations including Na⁺, Rb⁺, K⁺, Cs⁺, Ag⁺, Mg²⁺, Ba²⁺, Cd²⁺, Hg²⁺, Pb²⁺, and Al³⁺ (as their perchlorate salts) on the fluorescence spectra of **1** were also tested. As depicted in Figure 8, Pb²⁺ also leads to a similar, but smaller, fluorescence increase for **1** as did the Hg²⁺. Among these metal cations, Al³⁺ resulted in an obviously different fluorescence change. Addition of 100 equiv of Al³⁺ induced a strong emission of the pyrenyl excimer but a weak rhodamine emission, implying that Al³⁺ prefers the formation of a pyrenyl excimer but not the ring-opening of spirolactam for the rhodamine. This can be rationalized by two different binding structures of **1**: tren-spirolactam and tren-diamide units. In the presence of Hg²⁺, the metal ion interacts with the tren-spirolactam unit and induces ring-opening of the rhodamine to produce FRET-ON. On the other hand, Al³⁺ prefers to coordinate with the tren-diamide unit, leading to an enhanced pyrenyl excimer emission. However, this process does not open the spirolactam unit of the rhodamine moiety, and energy transfer cannot take place. These two different modes of action are illustrated in Figure 9.

The effects of some coexisting cations, including Na⁺, Rb⁺, Ba²⁺, Ca²⁺, Sr²⁺, Co²⁺, Zn²⁺, Pb²⁺, Ag⁺, Cd²⁺, and Al³⁺, on Hg²⁺ detection were also determined. As can be seen in Figure 10, addition of Hg²⁺ to a mixture of **1** with other metal ions

species except for Al³⁺ gives an increased rhodamine emission more than 7-fold, which is obviously due to a favorable and selective binding of the Hg²⁺ to the tren-spirolactam unit of **1**. Thus, Hg²⁺-selective binding and FRET-ON can take place in the competitive coexisting metal ions as well. In contrast, no significant fluorescence change of the **1**·Al³⁺ complex was observed upon addition of Hg²⁺, indicating that Al³⁺ was more tightly bound to the tren-diamide functional groups than to the tren-rhodamine group. In a reverse way, when the Al³⁺ was added to a solution of the **1**·Hg²⁺ complex (Figure 11), the pyrenyl emission band gradually revived while the rhodamine emission concomitantly declined, implying a diminished FRET process.

Conclusions

The synthesis and fluorescent properties of calixarene-based chemosensor **1**, which functions as Hg²⁺-induced FRET from the pyrenyl excimer (energy donor) to rhodamine (energy acceptor), are described. Addition of Hg²⁺ to a CH₃CN solution of ligand **1** gives a significantly enhanced fluorescence emission (FRET-ON). The FRET-ON process is also observed in the presence of competing metal ions. To the best of our knowledge, this is the first case of a calixarene-rhodamine-based FRET fluorescent chemosensor.

Experimental Section

Synthesis. Compounds **4**¹⁶ and **5**¹⁷ were prepared according to literature methods.

Preparation of 1. A solution of **3** (52 mg, 0.090 mmol), **6** (200 mg, 0.020 mmol), and CH₃OH/toluene (1:1, 5 mL) was refluxed for 24 h. After evaporation of the solvents in vacuo, the residue was chromatographed on silica gel CH₂Cl₂/acetone (17:3) as eluent to give **1** as a yellowish solid in 17% yield. Mp = 248–250 °C. ¹H NMR (300 MHz, CDCl₃): 9.14 (t, 2H, *J* = 3.6 Hz, *NH* amide), 8.39 (t, 2H, *J* = 4.8 Hz, *NH* amide), 8.30–7.84 (m, 18H, pyrene-*H*), 7.79–7.71 (m, 2H, rhodamine-*H*), 7.45–7.38 (m, 2H, rhodamine-*H*), 6.95 (s, 4H, ArOH), 6.73 (d, 4H, *J* = 2.4 Hz, ArH), 6.60 (s, 4H, ArH), 6.55 (d, 4H, *J* = 1.8 Hz, ArH), 6.42 (s, 2H, rhodamine-*H*), 6.40 (d, 2H, *J* = 2.1 Hz, rhodamine-*H*), 6.24 (d, 1H, *J* = 1.2 Hz, rhodamine-*H*), 6.22 (d, 1H, *J* = 2.7 Hz, rhodamine-*H*), 5.30 (d, 4H, *J* = 3.3 Hz, NHCH₂pyrene), 4.72 (s, 4H, OCH₂CO), 4.16 (s, 4H, OCH₂CO), 4.08 (d, 4H, *J* = 13.2 Hz, AB system, ArCH₂-Ar), 3.31–3.04 (m, 14H, CH₂CH₂ and ArCH₂Ar), 2.78 (d, 4H, *J* = 13.5 Hz, A'B' system, ArCH₂Ar), 3.32 (q, 8H, *J* = 5.1 Hz, CH₂-CH₃), 2.49 (t, 4H, *J* = 5.4 Hz, CH₂CH₂), 2.30 (t, 2H, *J* = 6.9 Hz, CH₂CH₂), 1.15–1.05 (m, 48H, *tert*-butyl, CH₂CH₃), 0.90 (s, 18H, *tert*-butyl), 0.87 (s, 18H, *tert*-butyl). ¹³C NMR (75 MHz, CDCl₃): 168.5; 168.2; 167.5; 153.4; 149.3; 149.0; 148.6; 147.5; 141.8; 132.4; 132.1; 131.0; 130.9; 130.6; 127.9; 127.2; 126.8; 126.3; 125.8; 125.; 125.2; 124.8; 124.7; 124.5; 108.1; 105.8; 98.0; 74.6; 64.8; 53.2; 44.1; 42.8; 37.3; 33.9; 33. 8; 33.5; 32.0; 31.5; 31.1; 30.8; 12.6. MW = 2491.31 g mol⁻¹ calcd for C₁₆₄H₁₈₄N₈O₁₄. MALDI-TOF: *m/z* = 2490.38. Analysis calcd: C, 79.07; H, 7.44. Found: C, 78.43; H, 7.71.

Preparation of 2. Using the same reaction conditions as for **1**, **3** (100 mg, 0.175 mmol), **6** (252 g, 0.35 mmol), and CH₃OH/toluene (1/1, 3 mL) were refluxed for 35 h. After evaporation of the solvents in vacuo, the crude mixture was chromatographed on silica gel with CH₂Cl₂/acetone (9:1) as eluent to give **2** as a light pink solid in 29% yield. Mp = 261–263 °C. ¹H NMR (300 MHz, CDCl₃): 8.87 (t, 2H, *J* = 5.1 Hz, *NH* amide), 7.91–7.85 (m, 2H, rhodamine-*H*), 7.49–7.39 (m, 2H, rhodamine-*H*), 7.07 (s, 8H, ArH), 7.05 (s, 4H, ArH), 6.99 (s, 4H, ArH), 6.45 (d, 2H, *J* = 2.1 Hz, rhodamine-*H*), 6.42 (s, 2H, rhodamine-*H*), 6.21 (d, 1H, *J* = 2.4 Hz, rhodamine-*H*), 6.18 (d, 1H, *J* = 2.7 Hz, rhodamine-*H*), 4.66 (s, 4H, OCH₂-

CO), 4.37 (d, 4H, $J = 12.9$ Hz, AB system, ArCH₂Ar), 4.28 (d, 4H, $J = 13.5$ Hz, A'B' system, ArCH₂Ar), 3.46–3.42 (m, 6H, CH₂CH₂), 3.40 (d, 8H, $J = 13.5$ Hz, AB and A'B' systems, ArCH₂-Ar), 3.31 (q, 8H, $J = 6.9$ Hz, CH₂CH₃), 2.81 (t, 4H, $J = 5.1$ Hz, CH₂CH₂), 2.46 (t, 2H, $J = 6.6$ Hz, CH₂CH₂), 1.25 (s, 18H, *tert*-butyl), 1.24 (s, 36H, *tert*-butyl), 1.20 (s, 18H, *tert*-butyl), 1.14 (t, 12H, $J = 6.9$ Hz, CH₂CH₃). ¹³C NMR (75 MHz, CDCl₃): 168.7; 167.9; 153.5; 153.2; 149.9; 148.8; 148.3; 148.2; 147.6; 143.5; 143.1; 133.2; 132.2; 131.6; 128.9; 128.1; 128.0; 127.8; 127.4; 126.5; 125.7; 123.8; 122.7; 108.2; 105.6; 97.9; 74.8; 65.2; 53.4; 53.2; 44.2; 37.6; 34.2; 34.0; 33.9; 32.9; 32.2; 31.5; 31.4; 31.2; 12.6. MW = 1949.68 g mol⁻¹ calcd for C₁₂₆H₁₅₉N₆O₁₂. MALDI-TOF: $m/z = 1948.19$. Analysis calcd: C, 77.62; H, 8.22. Found: C, 77.38; H, 7.91.

Preparation of 3. Rhodamine B (100 mg, 0.208 mmol) and N(CH₂CH₂NH₂)₃ (Tren) (610 mg, 4.16 mmol) were refluxed in CH₃-OH (2 mL) for 4 h. After evaporation of the solvents and several extractions in water–dichloromethane (with drying over sodium sulfate of the last crop of dichloromethane), **3** was separated as light orange oil in 79% yield. ¹H NMR (300 MHz, CDCl₃): 7.88–7.81 (m, 1H, rhodamine-*H*), 7.43–7.37 (m, 2H, rhodamine-*H*), 7.08–7.20 (m, 1H, rhodamine-*H*), 6.39 (s, 2H, Ar*H*), 6.36 (s, 2H, rhodamine-*H*), 6.25 (d, 1H, $J = 2.4$ Hz, rhodamine-*H*), 6.22 (d, 1H, $J = 2.7$ Hz, rhodamine-*H*), 3.17–3.07 (m, 2H, CH₂CH₂), 3.31 (q, 8H, $J = 7.2$ Hz, CH₂CH₃), 2.51 (t, 4H, $J = 5.7$ Hz, CH₂CH₂), 2.32 (t, 4H, $J = 6.0$ Hz, CH₂CH₂), 2.26–2.18 (m, 2H, CH₂CH₂), 1.15 (t, 12H, $J = 7.2$ Hz, CH₂CH₃). ¹³C NMR (75 MHz, CDCl₃): 167.9; 153.5; 152.9; 148.8; 132.3; 131.5; 128.9; 128.1; 123.8; 122.7; 108.1; 105.6; 97.7; 65.1; 55.6; 53.3; 52.1; 44.3; 39.3; 38.1; 30.8; 12.5. MW = 570.77 g mol⁻¹ calculated for C₃₄H₄₆N₆O₂, (MALDI-TOF): $m/z = 571.202$. Analysis calcd: C, 71.55; H, 8.12. Found: C, 72.05; H, 8.71.

Preparation of 6. The monomethylester *p*-*tert*-butyl-calix[4]-arene **4** (1.140 g, 1.58 mmol), *N*-(1-pyrenylmethyl) chloroacetamide (**5**) (488 mg, 1.58 mmol), K₂CO₃ (219 mg, 1.58 mmol), and KI (excess) were refluxed in CH₃CN (4 mL) for 15 h. The solvent was then evaporated in vacuo, and the residue was extracted with water–dichloromethane. The organic layer was dried over sodium sulfate. After filtration and evaporation of the solvent in vacuo, the residue was chromatographed on silica gel with a CH₂Cl₂/acetone (19:1) as eluent to give **6** as a yellowish powder in 38% yield. Mp = 162–164 °C. ¹H NMR (300 MHz, CDCl₃): 9.45 (t, 1H, $J = 5.7$ Hz, NH amide), 8.48–7.78 (m, 9H, pyrene-*H*), 7.16 (s, 2H, ArOH), 6.96 (d, 2H, $J = 2.4$ Hz, Ar*H*), 6.92 (d, 2H, $J = 2.4$ Hz, Ar*H*), 6.77 (d, 2H, $J = 6.6$ Hz, Ar*H*), 5.50 (d, 2H, $J = 5.7$ Hz, CH₂pyr), 4.61 (s, 2H, OCH₂CO), 4.38 (s, 2H, OCH₂CO), 4.09 (d, 2H, $J = 13.2$ Hz, AB system, ArCH₂Ar), 4.05 (d, 2H, $J = 13.2$ Hz, A'B' system, ArCH₂Ar), 3.44 (s, 3H, OCH₃), 3.21 (d, 4H, $J =$

13.2 Hz, AB system and A'B' system, ArCH₂Ar), 1.27 (s, 18H, *tert*-butyl), 0.95 (s, 9H, *tert*-butyl), 0.93 (s, 9H, *tert*-butyl). ¹³C NMR (75 MHz, CDCl₃): 168.9; 168.7; 149.9; 149.5; 149.2; 141.9; 132.3; 132.1; 132.0; 127.6; 127.3; 127.2; 127.1; 127.0; 125.8; 125.6; 125.1; 125.0; 124.9; 124.8; 124.5; 123.0; 74.5; 71.7; 51.7; 41.6; 33.9; 33.7; 31.9; 31.6; 31.5; 30.8. MW = 992.30 g mol⁻¹ calculated for C₆₆H₇₃-NO₇, (MALDI-TOF): $m/z = 1015.09$ (**6** + Na⁺). Analysis calcd: C, 79.89; H, 7.41. Found: C, 80.01; H, 7.50.

General Procedure for Spectral Studies. UV/vis and fluorescence spectra were recorded with a S-3100 spectrophotometer and a RF-5301PC spectrophotometer, respectively. Stock solutions (1.00 mM) of the metal perchlorate salts were prepared in CH₃CN. Stock solutions of **1** and **2** (0.06 mM) were prepared in CH₃CN. For all measurements of fluorescence spectra, excitation was at 343 nm with excitation and emission slit widths at 3.0 nm. UV/vis and fluorescence titration experiments were performed using 6.0 μM solutions of **1** and **2** in CH₃CN and varying concentrations of the metal perchlorate in CH₃CN.

Crystal Structure Determination. The diffraction data were collected at 100(2) K on a Nonius Kappa-CCD area-detector diffractometer and processed with HKL2000.²³ The structure was solved by direct methods and refined by full-matrix least-squares on F^2 with SHELXTL.²⁴ All non-hydrogen atoms were refined with anisotropic displacement parameters. The hydrogen atoms bound to oxygen and nitrogen atoms were found on Fourier-difference maps. Crystal data for **6**·4CH₂Cl₂: C₇₀H₈₁Cl₈NO₇, $M = 1331.96$, monoclinic, space group $P2_1/c$, $a = 12.7203(11)$ Å, $b = 45.428(4)$ Å, $c = 11.6976(6)$ Å, $\alpha = 91.788(5)^\circ$, $V = 6756.3(9)$ Å³, $Z = 4$. A total of 815 parameters were refined on 12799 independent reflections out of 142740 measured reflections ($R_{\text{int}} = 0.068$), giving final indices $R1 = 0.085$, $wR2 = 0.271$, and $S = 1.33$.

Acknowledgment. This research was supported by the Centre Culturel Français in Tunisia. It was also supported by the SRC program (R11-2005-008-02001-0 (2007)).

Supporting Information Available: Additional spectral figures, NMR data, tables of crystal data, atomic positions and displacement parameters, anisotropic displacement parameters, bond lengths, and bond angles in CIF format. This material is available free of charge via the Internet at <http://pubs.acs.org>.

JO071226O

(23) Otwinowski, Z.; Minor, W. *Methods Enzymol.* **1997**, 276, 307.

(24) Sheldrick, G. M. SHELXTL, Version 5.1, Bruker AXS Inc., Madison, WI, 1999.